Production of γ-TiAl-Ingots by Aluminothermic Reduction of TiO_2 and Refining by ESR

Dipl.-Ing. Jan-Christoph Stoephasius, Prof. Dr.-Ing. Bernd Friedrich

RWTH Aachen University, IME Process Metallurgy and Metal Recycling
Intzestr. 3
52056 Aachen, Germany

Abstract

In the last years γ-TiAl got a high importance due to its corrosion resistance and low density. In the actual formula 1 racing cars γ-TiAl is used for valves. Increasing pressure to reduce production costs, brought different alternative processes to the Kroll-Process. One of them is the aluminothermic reduction of titanium oxide pigment.

Since very successful lab-scale experiments at IME, Aachen proofed the principle possibility of this process (including co-reduction of alloying element oxides like Nb_2O_5), a pilot scale reactor (200 kg input mixture) for aluminothermic production of cylindrical ingots (60 kg) was constructed. The local reaction rate of the aluminothermic reaction was measured with 336 sensors which were positioned in the input mixture. The results brought fundamental new information about the reaction behaviour of aluminothermic processes and show in detail the effect of increasing pressure as a result of decreasing fraction void.

For the first time a quotient pyrometer was connected via temperature resistant light conducting cable with the mould. Thus it was possible to measure the temperature of the melt immediately after the end of the reaction during flowing into the mould under protective atmosphere. This allows on the one hand optimisation of the thermo-chemical non-adiabatic calculation of the reactions and on the other hand controlling of constant process parameters.

The theoretical metal-slag equilibria during electro slag remelting with a Ca-CaF_2-slag and the process parameters deviated from these were calculated using FactSage®-Software tool. A PESR furnace is used to refine the ingots at 1 MPa to decrease evaporation losses of Ca. A long term research program has started to optimise the ESR process. Input of high grade titanium/ aluminium scrap before electro slag remelting and replacing titanium oxide pigment by rutile to gain low cost γ-TiAl are subject of these examinations.

Introduction

The continuous enhancement of the efficiency of turbine and automotive engines is achieved by increasing working temperature and decreasing of the moving masses. Both postulations can be performed by one group of alloys, the intermetallic γ-titanium aluminides. Beside their low density (3 800 to 4 400 kg/m³) the high Young's modulus (170 GPa at 600 °C) and yield strength (420 MPa at 600 °C), especially the good corrosion and creep resistance are the main advantages. In the high pressure compressors of turbine engines, nickel based super alloys can be replaced by γ-TiAl, since the application temperature of γ-TiAl is high enough and the oxidation resistance is much better compared to titanium. In formula one racing motors intake and exhaust valves are nowadays manufactured from γ-TiAl. This allows an increased rotational speed of actually more than 18 000 rpm. [8]

In spite of the above mentioned advantages the significance of γ-TiAl in the material world is rather low as can be seen in figure 1. Nearly all kinds of materials follow a production-price correlation which can be explained with the fact, that in general lower production costs allow bigger application areas. The deviation of gold can be explained with the still high strategic interest and the demand of jewellery industry. As can be seen even at the actual price the application of γ-TiAl is too low. The main reason is, that most of the potential application areas are not explored yet due to the young age of this material. Decreasing of the price would additionally strengthen the economic force to introduce γ-TiAl to new applications.

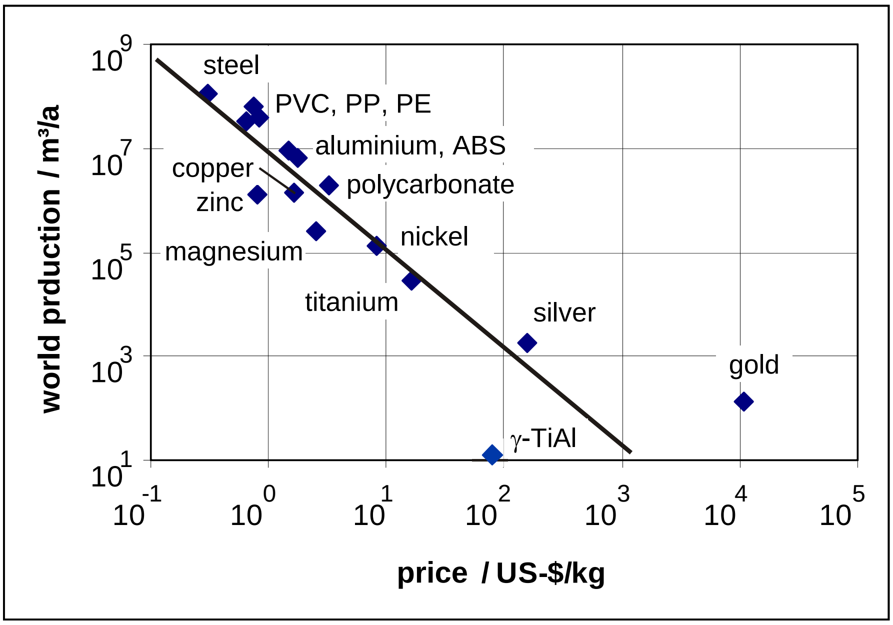

Figure 1: Position of γ-TiAl in the material world (state: 2001 - 2002, γ-TiAl: 2003)

The understanding of the high production costs of γ-TiAl is easier if the whole process route including the production of the alloying elements is considered (figure 2). Only aluminium is a commodity metal which is reduced from its oxide by electrolysis and granulated. Titanium is produced in the inefficient and expensive Kroll-process which indeed still has no industrial scaled alternative. The second disadvantage of the use of metallic titanium is the high strategic interest due to its military use. This leads to extreme variation of price and availability depending on the political and military situation of the world, as can be seen clearly nowadays. The alloying elements are usually added as master alloys. The alloying element oxides are reduced aluminothermically (ATR). Slag inclusions which typically occur during this process are separated during a second melting step (VIM) in a vacuum induction furnace. After casting the master alloys are crushed into a small size fraction.

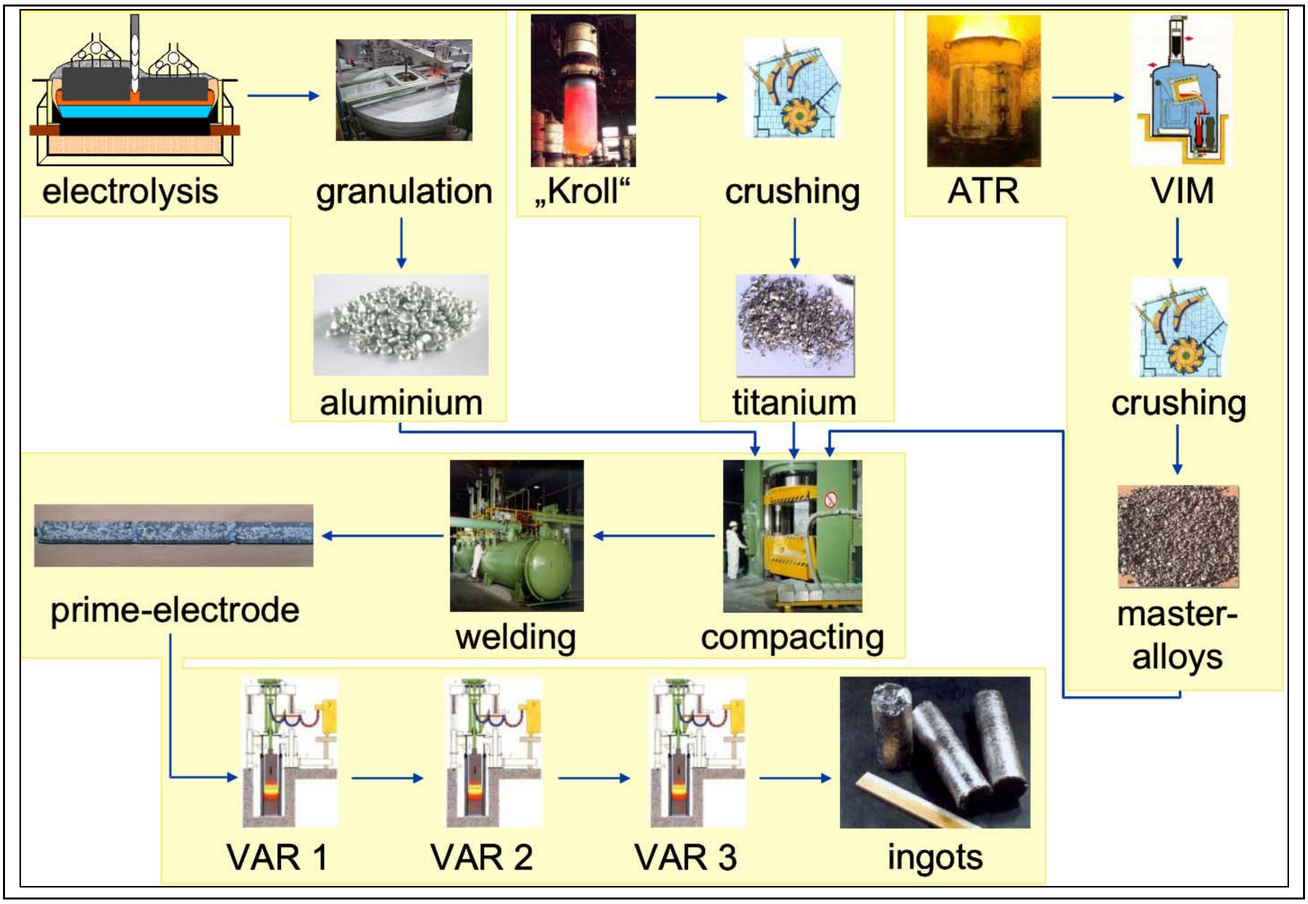

Figure 2: Conventional route for γ-TiAl-alloy production

Titanium, aluminium and the master alloys are mechanically mixed, compacted and welded to prime-electrodes under protective atmosphere. The prime-electrode is homogenized in a vacuum arc furnace. Due to the low homogenization ability of this process, the remelting must be repeated at least one time, but usually two times. [3, 4, 5] The analysis of this process route shows many disadvantages which lead to low process efficiency and high production costs:

1. Kroll-process:

- extensive equipment: Handling of liquid chlorides, Mg-electrolysis, small vacuum units, post distillation

- small high grade titanium yield (Fe contamination),
- small space related productivity,
- high energy consumption,
- mechanical removal of the Ti-sponge necessary,
- discontinuous.

2. Production of the prime electrode:
    - crushing of the homogenous input materials (contamination, costs),
    - nearly impossible adjusting of a homogeneous mix of the granules,
    - extensive compacting and welding technologies (contamination, costs).
3. Vacuum Arc Remelting (VAR):
    - high material quality necessary due to missing refining capabilities,
    - normally three remelting steps necessary due to low axial homogenisation,
    - mechanical cutting of the ingot necessary (head, foot and skull are inhomogeneous),
    - low material yield,
    - high energetic and manpower effort.

Development of the IME γ-TiAl-Process

The main idea of the new γ-TiAl-process which is developed at IME Process Metallurgy and Metal Recycling, department and chair of the RWTH Aachen University, is the use of industrialized procedures but with a significant reduction of the total process steps considering the entire production process. As can be seen in figure 3 the aluminium raw material changed slightly, since no granules but a powder is needed. Instead of titanium sponge the very competitive TiO_2-pigment is used as titanium source. The demand for alloying element raw materials didn’t change. The aluminothermic reduction which is worldwide used for the alloying elements in the conventional Ti-process is also used for the reduction of the TiO_2. [9]

While conventional aluminothermic reactors produce large blocks, that must be crushed, melted (typically VIM) and cast into ingots, the IME γ-TiAl-process fulfils this in a one-step in-line process. Immediately after the end of the aluminothermic reduction the metal flows into the mould through a bottom tap-hole. Before the reaction, the mould is filled with argon to prevent any nitrogen contamination of the ingot which in this case is the prime-electrode for the further remelting.

In opposite to the conventional process the IME prime-electrode has a high oxygen content due to the fact, that the reduction ability of aluminium is not high enough to deoxidize titanium to low oxygen contents. Therefore, instead of vacuum arc remelting the first remelting step is conducted in an inert gas electro slag remelting furnace (IESR) instead of the VAR. The advantage is, that a so-called active CaF_2-Ca-slag can be used as refining agent to reduce the oxygen content. Further a contamination of the metal with nitrogen from small leakages in the furnace as described in [6] can be avoided if an overpressure is used. Depending on the results of the IESR process and the demands of aviation industry a final VAR step can be proceeded to fulfil the certificate requirements.

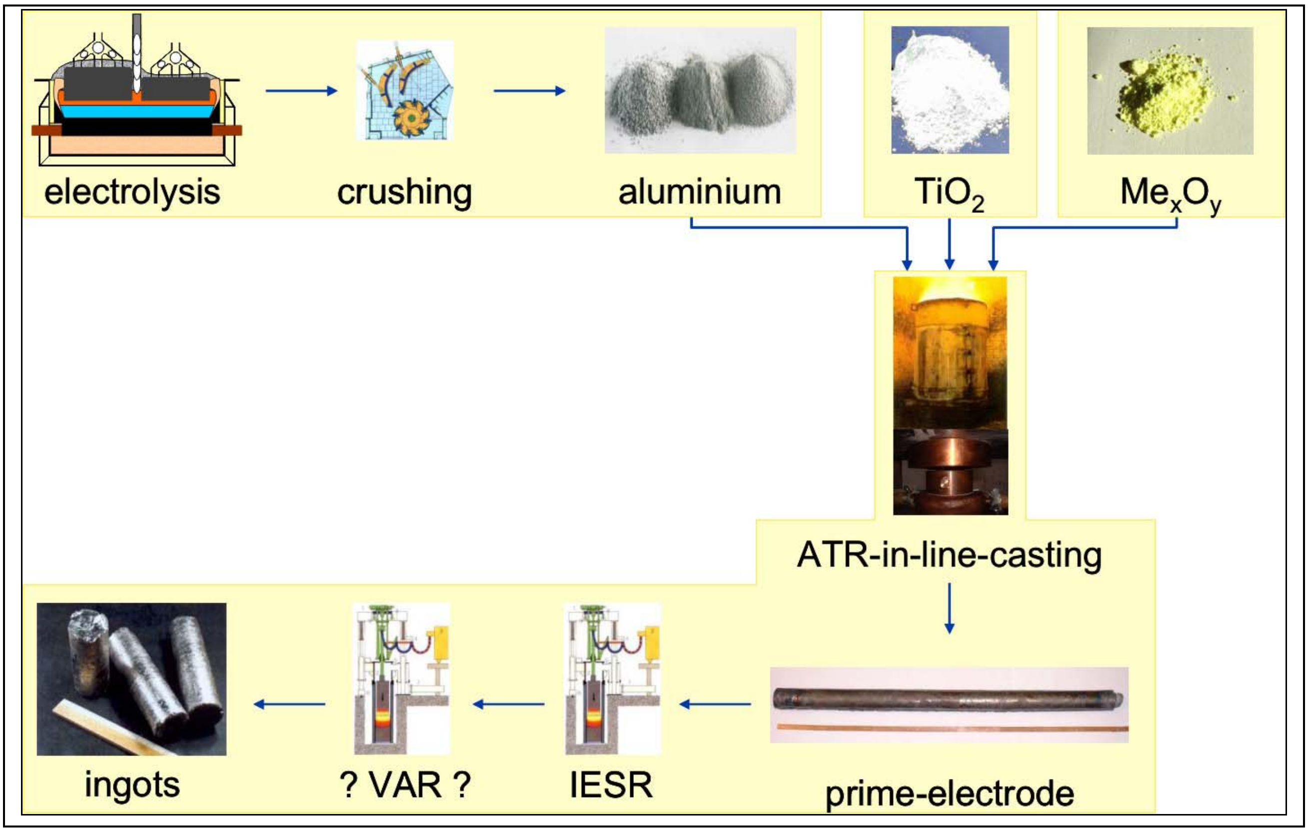

Figure 3: IME process for γ-TiAl-alloy production

The IME γ-TiAl-Process avoids nearly all mechanical treatment of the material, since neither crushing nor compacting is necessary. By reducing the process steps capital investment, process costs and energy consumption is reduced, a higher metal yield is expected and a lot of working force can be economized.

Modelling of the Aluminothermic Reduction

Conventional aluminothermic processes are mainly used for the production of master-alloys. Therefore, the tolerance of the ingot composition is much higher than for production of final alloys. Since the aluminothermic reduction is the final alloying step in the IME γ-TiAl-process and only small changes can be made during electro slag remelting by adding surcharges, the composition of the reaction mixture must be calculated extreme precisely considering final process temperature, metal slag equilibria, evaporation and flue dust losses.

Reaction Model

Earlier calculations were based only on thermochemical equilibrium calculations. Many kinetic and process based influences couldn't be taken into account. In [10] a new model was presented which allows description of the process based on nearly independent dimensionless parameters, that can be chosen according to thermochemical calculations and adjusted considering deviations of the experimental data. The reaction of each component of the reaction mixture is described by equation 1, where MeO is the metal oxide and R the reduction agent.

$$\begin{aligned}
&\mathrm{MeO}_{\nu_{O,Me,in}} + \left(r \cdot \eta_{Me} + RO\right) R \;\rightarrow \\
&\quad \left(\mathrm{Me}_{\eta_{Me}} \mathrm{R}_{\eta_{Me} \cdot r} \mathrm{O}_{(1-\eta_{O,Me}) \cdot \nu_{O,Me,in}}\right)_{\text{metal phase}} \\
&+ \left(\mathrm{Me}_{\eta_{Me,S}} \mathrm{R}_{(1-\eta_{R,G}) \cdot RO} \mathrm{O}_{\eta_{Me,S} \cdot \nu_{O,Me,S} + (1-\eta_{R,G}) \cdot RO \cdot \nu_{O,R,S}}\right)_{\text{slag phase}} \\
&+ \left(\mathrm{Me}_{\eta_{Me,G}} \mathrm{R}_{\eta_{R,G} \cdot RO} \mathrm{O}_{\eta_{Me,G} \cdot \nu_{O,Me,G} + \eta_{R,G} \cdot RO \cdot \nu_{O,R,G}}\right)_{\text{gas phase}} \\
&\text{with} \quad \eta_{Me,S} = 1 - \eta_{Me} - \eta_{Me,G} \\
&\quad RO = \frac{\nu_{O,Me,in} - (1-\eta_{O,Me}) \cdot \nu_{O,Me,in} - \eta_{Me,S} \cdot \nu_{O,Me,S} - \eta_{Me,G} \cdot \nu_{O,Me,G}}{\eta_{R,G} \cdot \nu_{O,R,G} + (1-\eta_{R,G}) \cdot \nu_{O,R,S}}
\end{aligned} \tag{1}$$

(η_{Me}: yield of the target metal [-]; $\eta_{Me,G}$: evaporation losses of the target metal [-]; $\eta_{O,Me}$: yield of the oxygen removal from the metal oxide [-]; $\eta_{R,G}$: evaporation losses of the reduction metal [-]; $\nu_{O,i,j}$: stoichiometric coefficient of the i-metal oxide in the phase j [-])

Equation 1 can be used to describe all side reactions (booster, brakes, slag surcharges, etc.), too. For pure booster reactions, e.g. $KClO_4$ or CaO_2, a metal yield $\eta_{Me} = 0$ and evaporation losses $\eta_{Me,G} = 1$ and $\eta_{Me,G} = 0$, respectively are chosen, since in the first case the reaction product is gaseous and in the second case completely in the slag phase. The typical slag surcharge is CaO. The metal yield η_{Me} is 0, since no metal phase is formed. In spite of this $\eta_{O,Me}$ is 1, since the oxygen is completely transferred into the slag phase. In this case RO is 0, i.e. the model doesn't demand any aluminium addition, because there is no (imagine) reduction reaction.

All yields η_i and stoichiometric coefficients ν_i are typical thermochemical parameters and can be calculated with thermochemical software like FactSage®. According to non-thermochemical effects like flue dust losses which occur due to the impact of exhausting offgases on not reacted mixture components, or not settled down metal droplets which lead to apparently lower metal yield, these parameters can be adjusted.

Propagation of the Reaction Front and Local Reaction Rates

One of the main factors during an aluminothermic reaction is the propagation of the reaction front during the process and the local reaction rate along the reaction front. The understanding of these factors can explain the typical behaviour of many metallothermic reactions, that after ignition up to about $^2/_3$ of the total reaction time the process runs extremely smooth, only few smoke and nearly no flames are visible (phase 1). After this time, there is a spontaneous strong increase in the reaction rate (phase 2). The smoke formation and flames become violent. Former explanation of this phenomenon was, that the mixture needs a long time to reach the final process temperature and therewith the maximum reaction rate. But this theory neither can explain the spontaneous increase in reaction rate nor the different “bulk ignition time” for different reactor scales. And as the temperature should increase constantly, the reaction rate should follow. Since the mixture is a very good thermal isolator, the total amount of mixture can’t influence the temperature in the middle of the reactor during ignition.

A new theory was developed which can explain the above described phenomena and reduces the danger of unexpected reaction rates, due to inadequate reactor geometry and fractional void of the mixture. It assumes, that there are two independent reaction phases with different reaction rates due to different pressure conditions in the bulk mixture. Depending on the size, density, ignition behaviour of the input material and the amount respectively viscosity of gaseous reaction products the first or the second phase predominates. Due to the large amount of gaseous reaction products but rather slow ignition behaviour, during aluminothermic production of γ-TiAl-x alloys both phases can be seen clearly. In the first phase of the total reaction time the gaseous products can move easily through the unreacted mixture and therefore, the pressure in the reaction front is rather low. Since the fractional void is very high, an increasing pressure forces melt to penetrate the unreacted mixture and increase the reaction rate. This happens in the second reaction phase, when there is not enough unreacted mixture left beside the reaction area to allow the produced gases to pass off. Instead they have to overcome the metallostatic pressure of the melt to move through it. Due to decreasing thickness the unreacted mixture beside the reaction front becomes mechanical instable and collapses.

An experimental set up was developed to proof this theory by measuring the propagation of the reaction front directly in a pilot scale reactor (ø 650 mm). In each corner of the reactor a backbone was installed over which the signal from 84 sensors was lead to the evaluation unit. The total amount of reaction mixture (here to produce γ-TiAl-Nb) was 180 kg. The results of this experiment are given in figure 4. It can be seen, that it takes 30 s after initial ignition to get the first response from the A and B backbone about 70 mm below the surface of the mixture. This is about 30 mm deeper than the igniting cap was positioned. This shows, that although the ignition reaction is strong exothermic and produces a large flame, there is no deep impact into the reaction mixture. For the next 60 s the reaction front moves slowly downwards. In the bottom part of the reacted area the reaction front moves sidewards with about half of the velocity in y-direction, while in the top part of the reacted area the propagation in x-direction is only very low. 90 - 110 s after ignition the signals become very indifferent (strong oscillation) in the top area of the reactor. The reason for this could be the throw-off of material which impacts the sensor cables. After this period the reaction rate increases significantly. Due to the higher reaction rate and the rising area of the reaction front, the amount of reacted material increases strongly. During the first 80 % of the total process time only 20 .. 25 % of the input material is reacted.

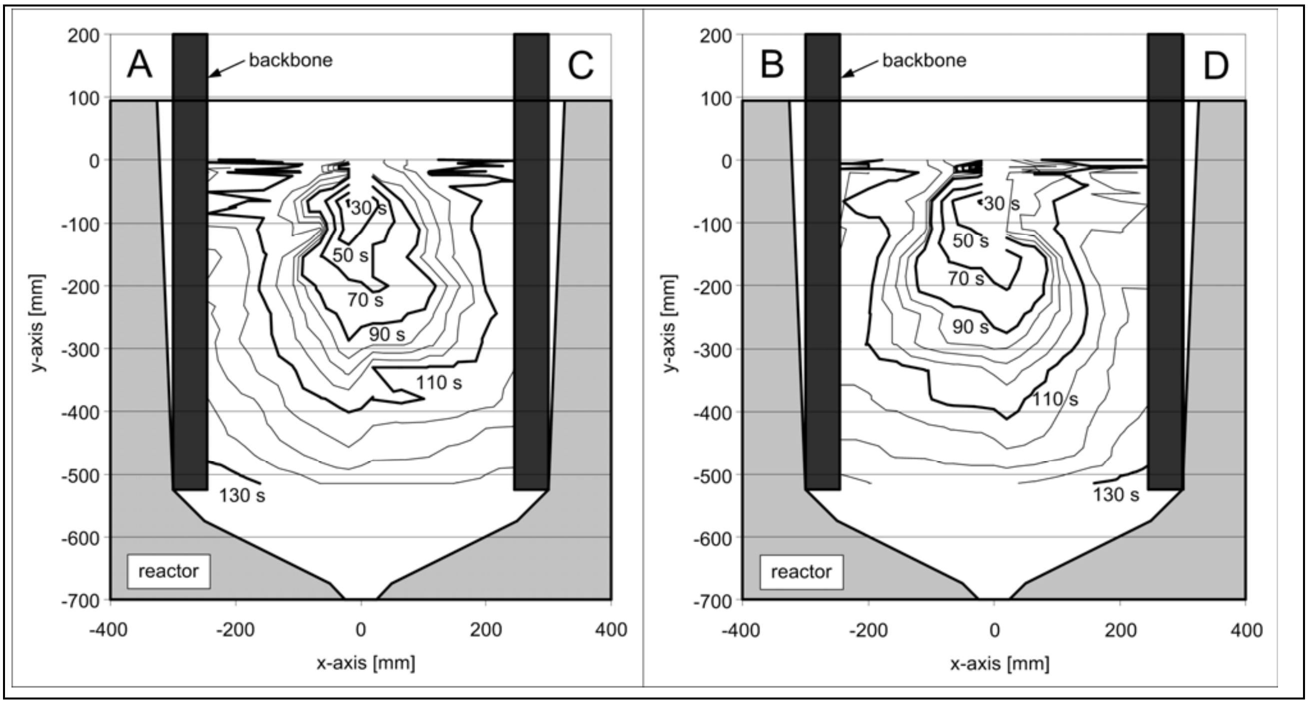

Figure 4: Propagation of the reaction front during the aluminothermic production of a γ-TiAl-Nb-alloy (two cross-sections of the reactor).

During the low velocity reaction phase the local reaction rate was 3,19 $^{mm}/_{s}$ and 3,7 $^{kg}/_{m^2s}$, respectively ($R^2 = 0{,}99$). During the high velocity reaction phase the local reaction rate was 7,47 $^{mm}/_{s}$ and 8,67 $^{kg}/_{m^2s}$, respectively ($R^2 = 0{,}97$). A detailed description of the work is given in [11].

Theoretical Process Temperature

As explained in [10], the target of an optimized ATR-process control is the adjusting of a constant process temperature, since this parameter is mainly responsible for melting of the components, metal-slag-separation and minimized evaporation. The calculation of the theoretical adiabatic process temperature can be fulfilled with thermochemical software. The temperature is reached, if the difference between the enthalpy of the reaction components in the initial state and the reaction products at process temperature is zero.

The calculations in the Ti-Al-Nb-O-system were fulfilled with FactSage® 5.3.1 [1] and the FACT 5.3, FToxid and 9329-Al-Nb-Ti-database. A theoretical adiabatic process temperature of 2 008 °C was obtained. During the process energy losses occur due to evaporating components, radiation of the melt surface and heat conduction into the lining material. The enthalpy of the evaporated components was calculated with FactSage® and is included in the theoretical adiabatic process temperature. The theoretical energy losses by radiation and heat conduction base on the measurement of the propagation of the reaction front. Considering the melt surface as function of the process progress the emitted power is nearly zero during the first 80 % of the total reaction time and increases in the second reaction phase up to 500 kW (figure 5). Integration of the radiation leads to a total emitted energy of 13,4 MJ. The energy losses by heat conduction are calculated with a one-dimensional insteady heat transfer simulation. Only a few mm of the lining material are significantly heated before the melt is tapped. Therefore, only about 7 MJ is lost by heat conduction. According to the energy losses the theoretical process temperature is 1 930 °C. A detailed description of the heat balance calculation has been published in [12].

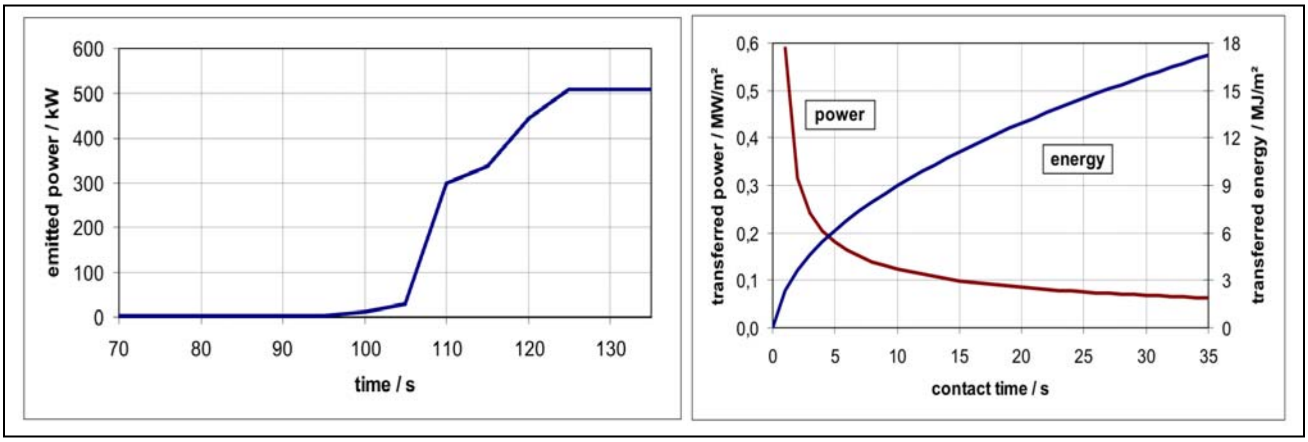

Figure 5: Emitted power losses of the reactor as function of the reaction time (left) and transferred power and total transferred energy as function of the contact time between melt and lining material (right) based on the measurements in [10] and the calculated adiabatic process temperature

Modelling of the Electro Slag Remelting

The ingot from the aluminothermic reduction process doesn’t fulfil the material requirements for the final γ-titanium aluminides due to three reasons. At first the oxygen content is much higher than postulated, since the reduction with aluminium doesn’t allow the production of low oxygen containing γ-titanium aluminides from thermochemical view. [2] Secondly on principle there is the possibility of small slag inclusions in the ingot from the aluminothermic reduction process which must be removed. Finally due to the slow cooling rate in the ceramic mould especially at high alloying element contents like niobium radial segregation effects may occur.

All these defects can be removed by electro slag remelting under protective atmosphere which is a common process for the production of nickel based super alloys. Because of the controlled melting and solidification conditions during this single remelting process a homogeneous microstructure is achieved. A special so-called active slag, this means a mixture of usually calcium fluoride and small amounts of a strong reducing agent like metallic calcium, can be used to remove the oxygen from the primary ingot.

Thermochemical Model

The thermochemical model, used for the calculation of the metal-slag-equilibria is based on the 9329-Al-Nb-Ti-, FACT53- and SGTE-databases (all provided from GTT Technologies, Herzogenrath, Germany) and the CaF_2-CaO-Ca-slag-model which is described in detail in [7]. The desoxidation reaction follows equation 2.

$$[\mathrm{TiO}]_{\mathrm{TiAl}} + [\mathrm{Ca}]_{\mathrm{Slag}} \rightarrow [\mathrm{Ti}]_{\mathrm{TiAl}} + [\mathrm{CaO}]_{\mathrm{Slag}} \qquad (2)$$

The final oxygen content in the metal phase is a function of the Ca- and CaO-content in the slag. Due to the stoichiometric coefficients of the desoxidation reaction, increasing Ca-content decreases the oxygen content according to a simple hyperbola. The influence of the CaO-content above 0,5 wt.-% is in the first approximation linear, but can better be described with a 3rd order polynomial. The theoretical oxygen contents, shown in figure 6, are calculated for the liquid-liquid-equilibrium between metal and slag. Below the solidus temperature the final oxygen content in the ingot is about 50 % lower (calculation at 1 500 °C) than in the liquid state. Experiments have to show, if this equilibrium is reached during electro slag remelting.

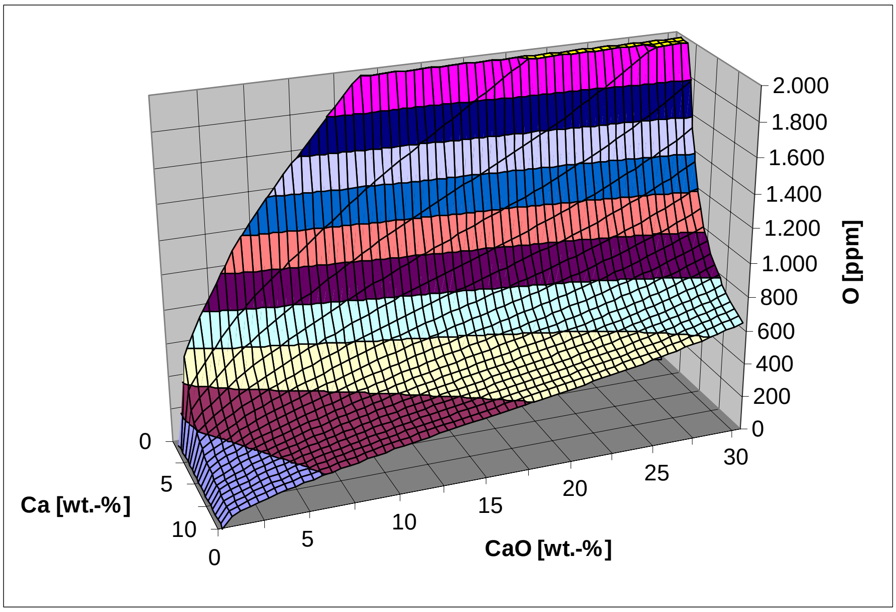

Figure 6: Theoretical oxygen content of a Ti-45Al-10Nb-alloy during electro slag remelting as function of the Ca- and CaO-content in the slag (ϑ = 1 600 °C, metal in liquid state)

Ca-Evaporation from the Active Slag

One of the main aims of electro slag remelting is the achieving of a homogeneous structure of the final ingot. Therefore, also the chemical composition must be constant along the axis. During the remelting process the slag is enriched with CaO from the desoxidation reaction. According to the CaO-content of the slag the Ca-content must be adjusted to receive a constant reduction potential and so a constant oxygen content in the final ingot. Due to the high partial pressure of Ca at process temperature significant Ca evaporation from the slag is expected. Since this is a non-equilibrium reaction, a kinetic model was developed to describe the Ca losses by diffusion. As can be seen in figure 7, the Ca atoms are transported by convection and diffusion into the slag diffusion layer, in which the further transport is only fulfilled by diffusion. After passing the slag / metal layer the Ca atoms diffuse through the gas diffusion layer and are finally transported by diffusion and convection through the gas phase. Alternatively, if the partial pressure of Ca is higher than the surrounding atmospheric pressure, Ca gas bubbles can form in the slag and transport the Ca directly into the gas phase.

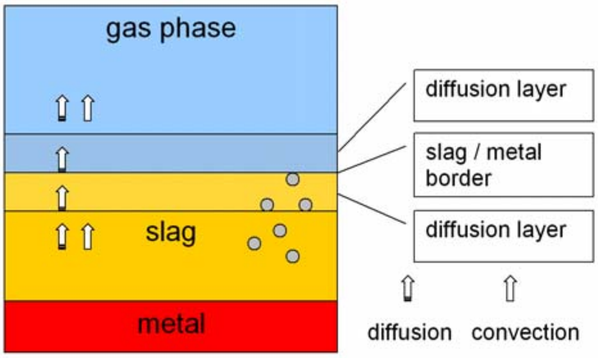

Figure 7: Schematic diagram of the transport layers and transport mechanism for the Ca evaporation (arrows: diffusion/ convection; circles: evaporation)

Due to the turbulent flow conditions in the slag, it can be assumed, that neither diffusion nor convection in the slag are evaporation limiting. A rough estimation of the evaporation rate at the slag / gas border according to the Hertz- Knudsen equation showed, that the evaporation rate is more than 1 000 times higher than observed in experiments and therefore can't be the transport limiting step. Therefore, the Ca losses are calculated according to a model, which assumes the diffusion in the gas diffusion layer and the combined diffusion and convection in the gas layer as transport limiting step according to equation 3 and 4. The modelled Ca evaporation as function of the total pressure is shown in figure 8.

$$D = \frac{3}{8} \cdot \sqrt{\frac{k^3 \cdot T_{g,m}^3}{\pi \cdot \mu \cdot \sigma^2}} \cdot \frac{1}{p_g} \qquad (3)$$

(D: diffusion coefficient [$^{m^2}/_{s}$]; k: Boltzmann’s constant [$1,38\cdot10^{-23}\ ^{J}/_{K}$]; $T_{g,m}$: av. gas temperature in the mould [K]; µ: reduced mass of Ca and Ar [kg]; σ: atom collision cross section [m²]; p_g: absolute gas pressure [Pa])

$$J_{Ca} = A\cdot D\cdot 0{,}15\cdot\sqrt[3]{\frac{g\cdot(T_{g,s}-T_{g,m})}{T_{g,m}\cdot\nu\cdot D}\cdot\left[1+\left(\frac{0{,}322\cdot D}{\nu}\right)^{11/20}\right]^{-20/11}}\cdot\frac{M_{Ca}\cdot p_{Ca}}{R\cdot T_{g,sl}} \qquad (4)$$

(J_{Ca}: Ca mass flow [kg/s]; A: slag surface [m²]; D: diffusion coefficient [$^{m^2}/_{s}$]; g: gravitational constant [$9{,}81\ ^{m}/_{s^2}$]; $T_{g,s}$: slag surface temperature [K]; $T_{g,m}$: av. gas temperature in the mould [K]; ν: cinematic viscosity of the gas phase [$^{m^2}/_{s}$]; M_{Ca}: molar mass of Ca [$^{kg}/_{mol}$]; p_{Ca}: partial pressure of Ca [Pa]; R: ideal gas constant [$8{,}314\ ^{J}/_{mol\cdot K}$])

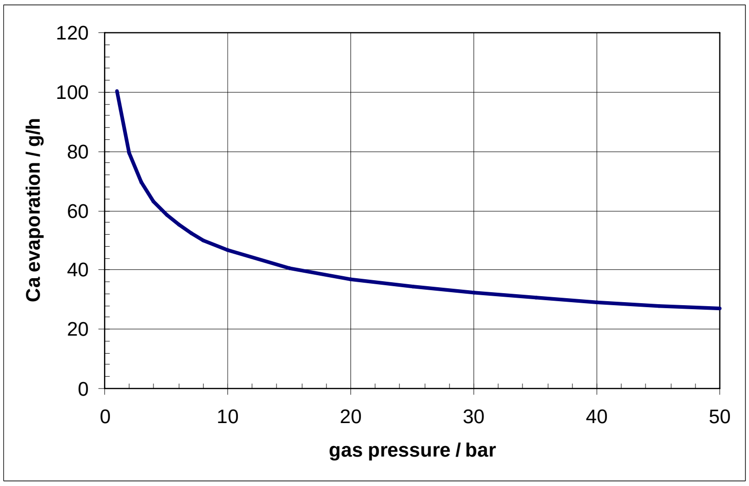

Figure 8: Theoretical Ca evaporation for a 5 wt.-% Ca containing CaF_2-slag at 1 720 °C ($ø_{mould}$ = 162,5 mm; $ø_{electrode}$ = 110 mm) for increasing Argon pressure in a PESR-furnace

Experimental

Based on previous results for the binary Ti-Al-system [7], in a first test series the thermochemical equilibria in the Ti-Al-Nb-system were analysed. The energy density of the reaction mixture was calculated with the Shemtchushny algorithm. In [10] we proposed, that a constant Shemtchushny factor doesn’t lead to a constant process temperature and herewith constant reaction behaviour, if the composition is changed. The qualitative analysis of the reaction intensity of these test series and the chemical analysis proofed this proposition. The first experiments were conducted with a Shemtchushny factor of 3 050 $^{J}/_{g}$. Although the energy density was not changed, increasing niobium content lead to more violent reactions. Therefore, after the 4 at.-% experiment the Shemtchushny factor was decreased to 3 000 $^{J}/_{g}$ and after the 9 at.-% experiment to 2 950 $^{J}/_{g}$. As can be seen in figure 9, this behaviour can be explained with the adiabatic process temperature of the reaction. Due to the lower heat capacity of niobium compared to titanium and aluminium, increasing niobium content leads to higher process temperature. Because of the lower difference in the molar heat capacity of the different metals, a constant Dautzenberg factor causes a lower but still not satisfying temperature increase during the test series. Future experiments will be conducted according to a constant adiabatic process temperature which should be 2 042 ±6 °C for a 20 kg laboratory scale.

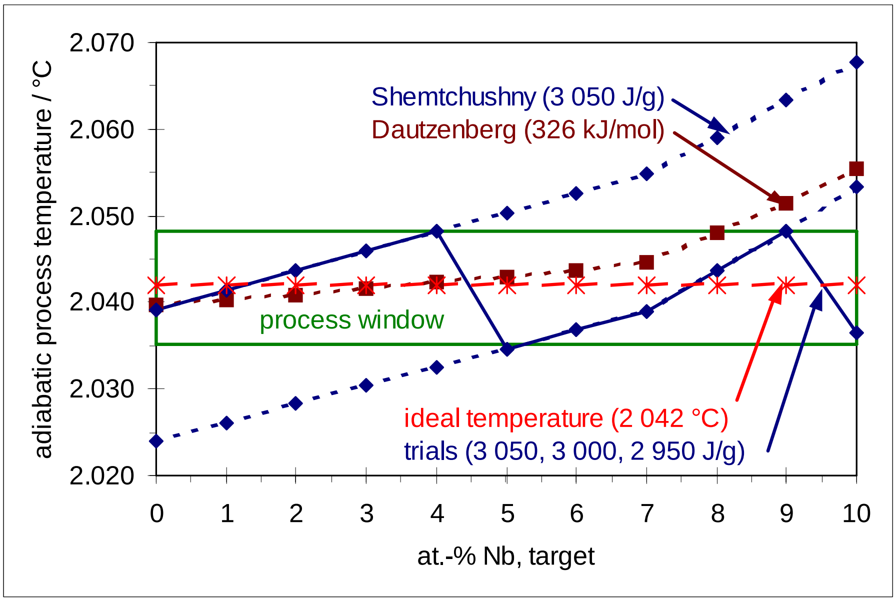

Figure 9: Adiabatic process temperature of the aluminothermic γ-TiAl-Nb production and thermal process window for 20 kg laboratory scale

The metal and slag analysis of the experiments are presented in figure 10. It can be seen, that the co-reduction of niobium could be fulfilled quite satisfying. Indeed strong segregation effects occurred at niobium contents above 8 at.-% which must be considered for further processing. The niobium losses in the slag were rather low (about 0,015 at.-%) at niobium contents below 6 at.-%. The calcium content in the slag was in general about 1 at.-% to low compared to the calculation. According to the theoretical propositions about the different reaction phases presented in [11] this can be explained with blown out calcium during the first reaction phase.

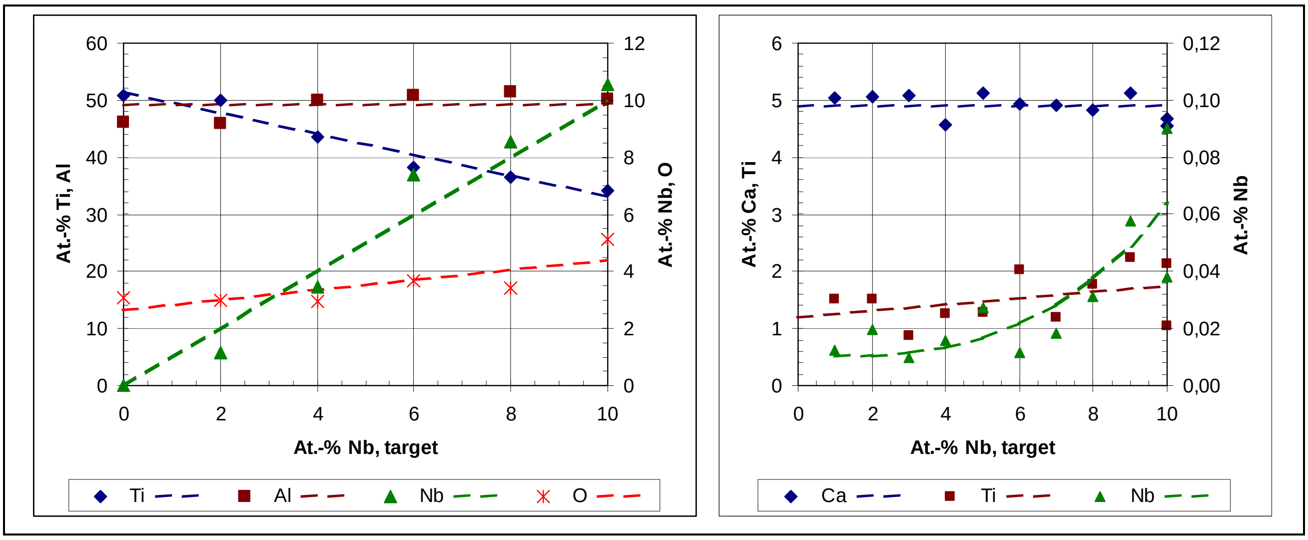

Figure 10: Metal (left) and slag (right) composition of aluminothermic reduced γ-TiAl-Nb

The theoretical heat balance was verified in a pilot scale experiment (180 kg reaction mixture) using a quartz fibre optics which was directly mounted into the downsprue of the mould and connected with a two-colour infrared pyrometer. The measured temperature was 1 920 °C which is in very good agreement with the calculated value (see above). A detailed description of the experiment is given in [12]. First experiments were successfully conducted to produce pilot scale prime-electrodes (50 .. 60 kg) which are actually analysed. The first produced γ-TiAl-Nb prime-electrode is shown in figure 11.

Figure 11: First produced pilot-scale γ-TiAl-Nb prime-electrode (dimensions: 113 x 1 320 mm) with connector for the stub of the electro slag remelting furnace on the left

Summary and Outlook

The main aim of the IME γ-TiAl process is the drastic reduction of the manufacture costs of γ-TiAl alloys by use of industrialized procedures and reduction of the total process steps considering the entire production process. A two step process route is used to reduce titanium oxide aluminothermically and refine the prime-material by electro slag remelting. Because the titanium aluminothermic reduction process is high sophisticated compared to conventional aluminothermic processes, many fundamental examinations of the reaction mechanisms were conducted to increase the understanding of this process. It could be shown, that it's possible to comply with the very small process window. Preparatory examinations for the refining of the prime-material by electro slag remelting were conducted, which allow the thermochemical modelling of the refining reactions as well as kinetic aspects of the remelting process and are the basis for a comprehensive process model of this process.

In actual test series the co-reduction of chromium and the reduction of high grade rutile is examined. The process stability of the aluminothermic reduction and the electro slag remelting is optimised. The mechanical properties of aluminothermic reduced ingots are tested, since if these tests show, that even a high oxygen containing γ-TiAl material fulfils the requirements for a commodity γ-TiAl, it would be possible to produce and process the alloys very economically. The standard aluminothermic reduction + VIM process route can be used in this case and instead of cold wall crucibles commercial ceramic crucibles are acceptable for all melting operations. The calcium evaporation from active CaF_2-Ca slags during electro slag remelting is examined using low alloyed steel electrodes. The results of these experiments will be presented separately.

Acknowledgments

The authors would like to acknowledge the Arbeitsgemeinschaft industrieller Forschungsvereinigungen "Otto von Guericke" e.V. (AiF) (Contract No. 14030 N) for support of the development of the IME-γ-TiAl-process with funds from the Bundesministerium für Wirtschaft und Arbeit (BMWA).

References

[1] BALE, C. W. ET AL. (2002): FactSage Thermochemical Software and Databases - Calphad, 26: 189-228, 2; Amsterdam.

[2] FRIEDRICH, B., HAMMERSCHMIDT, J. & STOEPHASIUS, J.-C. (2003): Aluminothermische Reduktion von Titanoxid - ERZMETALL **2**: 82-93; Clausthal-Zellerfeld.

[3] GÜTHER, V., OTTO, A., KESTLER, H. & CLEMENS, H. (Mar. 1999): Processing of Gamma-TiAl Based Ingots and Their Characterization. In: KIM, Y. W., DIMIDUK, D. M. & LORETTO, M. H. (Eds.): Gamma Titanium Aluminides 1999: 225-230; International Symposium on Gamma Titanium Aluminides, San Diego, ISBN 0-87339-451-8.

[4] GÜTHER, V. (2003): Herstellung von TiAl-Legierungsmaterial. In: DIETRICH, M. (Ed.): Titan-Aluminid-Legierungen - Eine Werkstoffgruppe mit Zukunft: 38-47; Forschungszentrum Jülich GmbH, Jülich, ISBN 3-89336-318-1.

[5] GÜTHER, V., CHATTERJEE, A. & KETTNER, H. (2003): Status and Prospects of γ-TiAl Ingot Production. In: CLEMENS, KIM, ROSENBERGER (Eds.): Gamma Titanium Aluminides 2003: 241-247; TMS, ISBN: 0-87339-543-3.

[6] GÜTHER, V., JOOS, R. & CLEMENS, H. (2002): Microstructure and defects in γ-TiAl based vacuum arc remelted ingot materials. In: HEMKER, K. J. & DIMIDUK, D. M. (Eds.): Third International Symposium on Structural Intermetallics: 167-173; TMS, ISBN: 0-87339-511-5.

[7] HAMMERSCHMIDT, J. (2003): Entwicklung einer Prozessroute zur Herstellung von γ-TiAl-Legierungen durch Aluminothermie und Schutzgas-Elektroschlackeumschmelzen; Aachen (Dissertation der RWTH Aachen, Shaker Verlag) - ISBN 3-8322-1971-4.

[8] JANSCHEK, P. (Dez. 2004): Titanaluminid - eine neue Werkstoffklasse für den Leichtbau in Flugtriebwerken und Hochleistungsmotoren - ThyssenKrupp techforum: 76-79; ThyssenKrupp AG, Düsseldorf, ISSN: 1612-2771.

[9] STOEPHASIUS, J.-C., FRIEDRICH, B. & HAMMERSCHMIDT, J. (2004): A new Processing Route for Titanium Alloys by Aluminothermic Reduction of Titanium Dioxide and Refining by ESR. - In: LÜTJERING, G. & ALBRECHT, J. (Ed.): Ti-2003 Science and Technology; Weinheim (Wiley-VCH-Verlag).

[10] STOEPHASIUS, J.-C. & FRIEDRICH, B. (2004): Modellierung metallothermischer Reaktionen – Berechnung der Einsatzmischung unter Berücksichtigung energetischer Effekte - World of Metallurgy - ERZMETALL, **4**: 177-184; Clausthal-Zellerfeld.

[11] STOEPHASIUS, J.-C. & FRIEDRICH, B. (2005): Modelling of Metallothermic Reactions (2) – Local Reaction Rates during Aluminothermic γ-TiAl-Nb Production - World of Metallurgy - ERZMETALL, **2**: 63-69; Clausthal-Zellerfeld.

[12] STOEPHASIUS, J.-C. & FRIEDRICH, B. (2005): Advances in Contactless Online-Temperature-Measurement with IR-Pyrometry - World of Metallurgy - ERZMETALL, **3**: 113-118; Clausthal-Zellerfeld.